Available online at www.sciencedirect.com
SCIENCE DIRECT®
Biochemical Pharmacology 67 (2004) 191–199
Biochemical Pharmacology
www.elsevier.com/locate/biochempharm

Evidence that unsaturated fatty acids are potent inhibitors of renal UDP-glucuronosyltransferases (UGT): kinetic studies using human kidney cortical microsomes and recombinant UGT1A9 and UGT2B7

Paraskevi Tsoutsikos[a], John O. Miners[a], Alan Stapleton[b], Anthony Thomas[c], Benedetta C. Sallustio[d], Kathleen M. Knights[a,*]

[a]*Department of Clinical Pharmacology, Flinders University and Flinders Medical Centre, Bedford Park, 5042 Adelaide, Australia*
[b]*Repatriation General Hospital, Daw Park, 5041 Adelaide, Australia*
[c]*Department of Anatomical Pathology, Flinders University and Flinders Medical Centre, Bedford Park, 5042 Adelaide, Australia*
[d]*Department of Cardiology and Clinical Pharmacology, The Queen Elizabeth Hospital, Woodville, 5011 Adelaide, Australia*

Received 2 July 2003; accepted 28 August 2003

Abstract

Renal ischaemia is associated with accumulation of fatty acids (FA) and mobilisation of arachidonic acid (AA). Given the capacity of UDP-glucuronosyltransferase (UGT) isoforms to metabolise both drugs and FA, we hypothesised that FA would inhibit renal drug glucuronidation. The effect of FA (C2:0–C20:5) on 4-methylumbelliferone (4-MU) glucuronidation was investigated using human kidney cortical microsomes (HKCM) and recombinant UGT1A9 and UGT2B7 as the enzyme sources. 4-MU glucuronidation exhibited Michaelis–Menten kinetics with HKCM (apparent K_m (K_m^{app}) 20.3 μM), weak substrate inhibition with UGT1A9 (K_m^{app} 10.2 μM, K_{si} 289.6 μM), and sigmoid kinetics with UGT2B7 (S_{50}^{app} 440.6 μM) Similarly, biphasic UDP-glucuronic acid (UDPGA) kinetics were observed with HKCM (S_{50} 354.3 μM) and UGT1A9 (S_{50} 88.2 μM). In contrast, the Michaelis–Menten kinetics for UDPGA observed with UGT2B7 (K_m^{app} 493.2 μM) suggested that kinetic interactions with UGTs were specific to the xenobiotic substrate and the co-substrate (UDPGA). FA (C16:1–C20:5) significantly inhibited (25–93%) HKCM, UGT1A9 or UGT2B7 catalysed 4-MU glucuronidation. Although linoleic acid (LA) and AA were both competitive inhibitors of 4-MU glucuronidation by HKCM (K_i^{app} 6.34 and 0.15 μM, respectively), only LA was a competitive inhibitor of UGT1A9 (K_i^{app} 4.06 μM). In contrast, inhibition of UGT1A9 by AA exhibited atypical kinetics. These data indicate that LA and AA are potent inhibitors of 4-MU glucuronidation catalysed by human kidney UGTs and recombinant UGT1A9 and UGT2B7. It is conceivable therefore that during periods of renal ischaemia FA may impair renal drug glucuronidation thus compromising the protective capacity of the kidney against drug-induced nephrotoxicity.

Keywords: UDP-glucuronosyltransferases; UGT1A9; UGT2B7; Human kidney microsomes; 4-Methylumbelliferone glucuronidation; Inhibition by fatty acids

1. Introduction

FA are predominantly straight-chain monocarboxylic acids ranging from 4 to 24 carbon atoms that may be either saturated or unsaturated. They are essential for integrated functioning of the human body, serving both as an energy source and as a unit for energy storage. Their importance, however, extends beyond their role in anabolic and catabolic pathways. FA *per se* act as regulatory molecules affecting enzyme activity (e.g. acetyl-CoA carboxylase) and gene transcription as endogenous ligands of peroxisome-proliferator-activated receptors [1]. In addition, FA are esterified in membrane phospholipids and are critical for the structure and hydrophobicity of mammalian cell membranes. While all FA contribute to membranous hydrophobicity, polyunsaturated FA additionally fulfil a unique role as precursors of potent signal molecules.

* Corresponding author. Tel.: +61-8-8204-4331; fax: +61-8-8204-5114.
E-mail address: Kathie.knights@flinders.edu.au (K.M. Knights).

Abbreviations: FA, fatty acid(s); UGT, UDP-glucuronosyltransferase; 4-MU, 4-methylumbelliferone; HKCM, human kidney cortical microsomes; MM, Michaelis–Menten; K_m^{app}, apparent Michaelis constant; S_{50}, substrate concentration at half-maximal velocity; UDPGA, UDP-glucuronic acid; LA, linoleic acid; AA, arachidonic acid.

0006-2952/$ – see front matter © 2003 Elsevier Inc. All rights reserved.
doi:10.1016/j.bcp.2003.08.025

Oxidative metabolism of FA produces prostaglandins, leukotrienes and hydroxy-fatty acids, collectively referred to as eicosanoids. These bioactive molecules are synthesised from 20-carbon polyunsaturated FA namely dihomo-γ-linolenic acid, eicosapentaenoic acid and AA. Eicosanoids synthesised from AA contribute to major pathophysiological conditions including chronic inflammatory diseases (e.g. rheumatoid arthritis, psoriasis) [2,3], toxic and immune mediated nephropathies [4], formation of thrombi and atheroma, and cell proliferation [5].

AA (C20:4$n-6$) is the most abundant polyunsaturated FA in membrane phospholipids and is liberated as a result of the action of phospholipases and mechanical or mitogenic stimuli. Free AA is rapidly metabolised by three enzyme systems: cyclo-oxygenases (COX), lipo-oxygenases (LOX) and cytochromes P-450 (CYP). Oxygenation of released AA *via* the action of COX produces prostaglandins of the 2-series (e.g. PGE_2) and thromboxanes; *via* the LOX pathway the 4-series leukotrienes (e.g. LTB_4) and hydroxy-fatty acids; and *via* CYP the epoxyeicosatrienoic acids (EETs) and their corresponding diols and hydroxyeicosatetraenoic acids (HETEs).

Carboxylic acids are common substrates for UGT (EC 2.4.1.17). Of the 27 known human *UGT* genes, 14 (UGT 1A1, 1A3, 1A4, 1A6, 1A7, 1A8, 1A9, 1A10, 2A1, 2B4, 2B7, 2B15, 2B17, and 2B28) encode proteins that are catalytically active towards a myriad of xeno- and endobiotics. The glucuronidation of medium chain FA and the unsaturated FA, LA, α-linolenic and AA by rat UGT2B1 was reported in 1994 [6]. Later studies demonstrated that monkey UGT2B9 (89% identical to human UGT2B7) and human UGT1A3 glucuronidated C2–C12, and C10 and C12 straight-chain saturated FA, respectively [7,8]. More recently, glucuronidation of LA, the immediate precursor of AA, by human liver microsomes and glucuronidation of the two naturally occurring metabolites of LA, 13-hydroxyoctadecadienoic acid (13-HODE) and 13-oxooctadecadienoic acid (13-OXO) by human UGT2B7, was reported [9–11]. Subsequent studies also established that AA, 20-HETE and PGE_2 were substrates for human hepatic and intestinal UGTs and recombinant UGT2B7 [12].

Although knowledge of xenobiotic metabolism is often based on studies using predominantly liver, significant glucuronidation activity towards endogenous and exogenous compounds has been reported for human kidney [13]. Substrates for renal UGTs include paracetamol, morphine, 4-MU, 1-naphthol, 4-nitrophenol, propofol, mycophenolic acid, hyodeoxycholic acid, estradiol and testosterone amongst others [14–16]. UGT activity is primarily localised to the cortical region and the isoforms identified in human renal tissue include 1A3, 1A6, 1A9, 2B4, 2B7, 2B10, 2B15 and 2B17 [17–19].

The physiological functions of the kidney are varied and numerous, and the metabolism of AA plays an important role in integrating renal dynamics in particular renal vascular tone, glomerular function and fluid and electrolyte balance. Although the concentration of free AA in resting cells is universally described as 'low', once released the concentration can range from 10 to 100 μM [20]. Progression to acute renal failure is also accompanied by increased intracellular accumulation of FA. Since most UGT isoforms are capable of metabolising both drugs and endobiotics, we hypothesised that FA would inhibit renal drug and chemical glucuronidation. In order to assess the potential effects of FA on renal glucuronidation, we utilised 4-MU as the probe UGT substrate and HKCM and recombinant UGT1A9 and UGT2B7 as the enzyme sources. UGT1A9 and UGT2B7 were selected for investigation as both are known to be expressed in human kidney [17,18] and both have the capacity to glucuronidate substrates containing a carboxylic acid function, a characteristic chemical feature of FA [17]. Accordingly, the inhibitory effect of a range of saturated (C2–C20) and unsaturated (C14:1–C20:5) FA on 4-MU glucuronidation by HKCM and recombinant UGT1A9 and UGT2B7 was determined.

2. Materials and methods

2.1. Materials

The following compounds were purchased from Sigma-Aldrich: UDPGA, 4-MU, 4-MU–β-D-glucuronide and the FA (either as the free acid or the sodium salt) acetic (C2:0), butyric (C4:0), *n*-caproic (C6:0), caprylic (C8:0), capric (C10:0), myristic (C14:0), myristoleic (C14:1), palmitic (C16:0), palmitoleic (C16:1), stearic (C18:0), oleic (C18:1), linoleic (C18:2), α-linolenic (C18:3), arachidic (C20:0), gondoic (C20:1), eicosadienoic (C20:2*n*6), dihomo-γ-linolenic (C20:3), arachidonic (C20:4), eicosapentaenoic (C20:5). Fatty acids were dissolved in ethanol (100% analytical grade) and stored desiccated in amber glass vials at −20°. Purity of the solutions as determined by GC (data not shown) was >99.5% over a 3-month period. All other chemicals were of the highest analytical grade available and obtained from commercial sources.

2.2. Human kidney tissue

Human kidney tissue from six subjects who had undergone radical nephrectomy for malignant disease was obtained from the joint Flinders Medical Centre/Repatriation General Hospital Tissue Bank, Adelaide, South Australia. Approvals for tissue collection and *in vitro* xenobiotic metabolism studies were obtained from the Research and Ethics Committee of the Repatriation General Hospital and the Flinders Clinical Research Ethics Committee, Flinders Medical Centre, South Australia. Renal cortical tissue distant to the primary tumour was isolated from fresh kidneys immediately following surgery

Table 1
Human kidney donor details and tissue histology

Tissue code	Gender	Age (years)	Drug history	Histology
K1	M	73	Ranitidine	Not available
K3	M	79	Acetylsalicylic acid	Benign nephrosclerosis, mild hypertensive-like vascular change but no evidence of primary glomerular disease
K4	M	83	Amitriptyline, paracetamol	Benign hypertensive-like vascular change, foci of tubular atrophy and inflammation. No primary glomerular disease
K5	M	72	Diclofenac, doxepin	Mild focal benign nephrosclerosis consistent with age of patient. No significant abnormality
K6	M	80	Lansoprazole, acetylsalicylic acid, allopurinol	Mild benign nephrosclerosis with no evidence of primary glomerular disease, consistent with age of patient
K7	M	43	Omeprazole, dexamethasone	Minimal glomerulosclerosis and focal interstitial inflammation. Mild hypertensive-like vascular changes, no significant interstitial scarring

and samples were either placed in 10% neutral phosphate buffered formalin for routine histology, used immediately for the preparation of microsomes, or cryopreserved (−70°) for later studies. Representative tissue samples were examined by a specialist histopathologist (AT). Only age related benign nephrosclerosis and, hypertensive-like vascular changes were reported and all sections were confirmed as cortex free of medulla. Relevant details of the donors and tissue histology are summarised in Table 1.

2.3. Preparation of renal cortical microsomes

HKCM were prepared using a standard differential ultracentrifugation technique [16] with minor modifications. Cortical tissue was homogenised initially using an Ultra-Turrax (max 60 s) in 0.25 M sucrose/2 mM Tris (pH 7.5) followed by three passes with a Potter–Elvehjem homogeniser and then centrifuged (4°) at 600 *g* for 10 min followed by 10,000 *g* for a further 10 min. The supernatant fraction was removed, the pellet resuspended in 10 mM Na_2HPO_4/1.15% KCl (pH 7.4) and centrifuged 100,000 *g* for 60 min. The microsomal pellet was resuspended in 0.1 M Na_2PO_4 (pH 7.4)/20% (w/v) glycerol, analysed for protein concentration [21] and stored at −70°.

2.4. Expression of UGT1A9 and UGT2B7

UGT1A9 and UGT2B7 were stably expressed in human embryological kidney 293T (HK293) cells (ATCC). Cells were transfected separately with the UGT1A9 and UGT2B7 cDNAs cloned into the expression vector pEF-IRES-puro-6 and selected with puromycin [22]. Microsomes were prepared from cells expressing UGT1A9 as described previously [23]. As microsome preparation resulted in loss of activity of UGT2B7, harvested cells were resuspended in storage buffer (100 mM K_2HPO_4/1 mM EDTA/0.5 mM dithiothreitol) and cell lysate prepared by probe sonication using four 1 s bursts interspersed by 3 min cooling on ice. The lysate was centrifuged briefly (12,000 *g* × 5 min) and the supernatant fraction stored at −70° until required for activity studies.

2.5. Quantification of 4-MU glucuronide formation

A modified fluorescence assay described previously by Miners *et al.* [24] was used for quantification of 4-MU glucuronide formation by HKCM, UGT1A9 and UGT2B7. Preliminary studies established both the conditions for linearity of the reaction with respect to time and protein concentration, and that substrate consumption during the course of the incubation was less than 10%. The standard incubation medium to determine the kinetics of 4-MU glucuronidation comprised 0.1 M KH_2PO_4 (pH 7.4), 5 mM $MgCl_2$, UDPGA (HKCM 2.5 mM; UGT1A9 and UGT2B7 5 mM), 4-MU 0–0.2 mM for HKCM and UGT1A9; 0–2 mM for UGT2B7 and protein (HKCM and UGT1A9 0.017 mg/mL; UGT2B7 0.033 mg/mL) in a total volume of 0.6 mL. HKCM samples were incubated (37°) for 20 min while the duration of the incubation for UGT1A9 and UGT2B7 was 45 min. Reactions were terminated by the addition of 0.6 M glycine–0.4 M trichloroacetic acid (0.14 mL) and cooling on ice. Incubation mixtures were extracted with chloroform and the fluorescence of 4-MU glucuronide in the aqueous phase determined at 365 nm using an excitation wavelength of 315 nm. Quantification was undertaken by reference to standard curves prepared using 4-MU glucuronide concentrations in the range of 0–10 μM. Experiments to determine the apparent K_m (K_m^{app}) for UDPGA were undertaken as described using HKCM, UGT1A9 and UGT2B7 with the following changes; the concentration of 4-MU was fixed (0.5 mM) and the concentration of UDPGA varied from 0.01 to 5 mM for HKCM, and 0.05–7.5 mM for UGT1A9 and UGT2B7.

2.6. Inhibition of UGT activity by FA

Initially a range of FA C2–C20:5 (10 μM) dissolved in ethanol (final concentration 1% v/v) were screened for an inhibitory effect on 4-MU glucuronidation catalysed by HKCM, UGT1A9 and UGT2B7. For these studies, the concentration of 4-MU corresponded to the apparent K_m/s_{50}; viz. 0.02 mM for HKCM, 0.01 mM for UGT1A9 and 0.45 mM for UGT2B7. Kinetic studies were undertaken

to determine apparent K_i values where significant inhibition was observed. The FA investigated subsequent to the initial screening study included LA (C18:2) and AA (C20:4). The source of UGT protein was HKCM and UGT1A9 and the effect of the individual FA was investigated using varying concentrations of 4-MU (0.01–0.06 mM) and either C18:2 (1–8 μM) or C20:4 (0.02–0.2 μM).

2.7. Kinetic and statistical analyses

Data points for HKCM represent the mean of five to six individual kidneys each studied in duplicate. For UGT1A9 and UGT2B7 data represent the mean of duplicate estimations. The kinetic parameters s_{50}, K_m^{app}, V_{max} and K_i were derived from untransformed data fitted using an extended least squares modelling program (EnzFitter, Biosoft). Equations used included: Michaelis–Menten (MM) for single- and two-enzyme systems, substrate inhibition and the Hill equation [25]. All data were analysed using simple (robust) weighting and the kinetic parameters are reported as mean ± SE of the parameter estimate. The goodness of fit was determined from the analysis of variance for the curve fit, r^2 values and standard error estimates [26]. Statistical significance of the effect of FA on 4-MU glucuronidation by HKCM was determined using a univariate ANOVA (SPSS v 11.5) with factors FA and kidney, and with Scheffè *post hoc* tests. The combined kidney–FA interaction was not significant and was removed from the model. Values of $P < 0.05$ were considered statistically significant.

3. Results

3.1. UDPGA kinetics

The kinetic parameters for the co-substrate UDPGA and for glucuronidation of 4-MU were studied using HKCM and recombinant UGT1A9 and UGT2B7. In the presence of a fixed concentration of 4-MU (0.5 mM) apparent biphasic Eadie–Hofstee plots were observed for UDPGA when using HKCM (Fig. 1A) and UGT1A9 (Fig. 1B). The data for HKCM were best fitted to the Hill equation with $h < 1$, indicative of negative co-operativity (Table 2). The apparent s_{50} for individual kidneys ranged from 259.1 to 416.9 μM, with a Hill coefficient in the range of 0.7–0.8. From the composite fit of all data (five kidneys each studied in duplicate) the s_{50} (UDPGA) and h were 354.3 ± 17.9 μM and 0.75 ± 0.015, respectively. Similar to HKCM, the UDPGA kinetic data for UGT1A9 were best modelled by the Hill equation; s_{50} 88.2 ± 1.018 μM. V_{max} 4.1 ± 0.01 nmol/min/mg and h 0.8 ± 0.009. In contrast, linear kinetics for UDPGA (Fig. 1C) consistent with a MM model were observed for UGT2B7 with K_m^{app} 493.2 ± 0.1 μM and V_{max} 0.5 ± 0.00003 nmol/min/mg.

3.2. Kinetics of 4-MU glucuronidation

4-MU glucuronidation by HKCM conformed to a single enzyme MM model (Fig. 1D). From the fit of all data (six kidneys each studied in duplicate) the K_m^{app}, V_{max} and CL_{int} values were 20.3 ± 0.03 μM, 8.7 ± 0.005 nmol/min/mg and 428.5 μL/min/mg, respectively. Data from the individual kidneys displayed a 1.4-fold variation in the apparent K_m and a 2-fold variation in V_{max} (Table 2). 4-MU glucuronidation by UGT1A9 was characteristic of substrate inhibition (Fig. 1E). However, inhibition was minor as the K_{si} (289.6 ± 12.9 μM) was ~28-fold greater than the apparent K_m for 4-MU, viz. 10.2 ± 0.29 μM. In contrast, 4-MU glucuronidation by UGT2B7 exhibited sigmoidal kinetics indicative of positive homotropic cooperativity (Fig. 1F) with an apparent s_{50} of 440.6 ± 14.3 μM, V_{max} 1.02 ± 0.02 nmol/min/mg and Hill coefficient h 1.65 ± 0.062.

3.3. Effect of FA on 4-MU glucuronidation

Saturated FA (C2–C20) and the monoenoic FA myristoleic acid (C14:1) had no statistically significant effect on

Table 2
Kinetic parameters for 4-MU glucuronidation and the co-substrate UDPGA using HKCM

Kidney tissue code	Kinetic parameters (±SE)[a]				
	4-MU glucuronidation			UDPGA	
	K_m (μM)	V_{max} (nmol/min/mg)	CL_{int} (μL/min/mg)	s_{50} (μM)[b]	h[c]
K1	18.9 ± 0.7	8.4 ± 0.1	443.5	416.9 ± 38.6	0.7 ± 0.02
K3	25.1 ± 0.7	7.9 ± 0.1	315.6	–	–
K4	23.5 ± 0.2	7.7 ± 0.02	326.2	382.1 ± 17.9	0.8 ± 0.02
K5	18.8 ± 0.6	12.8 ± 0.1	679.5	353.8 ± 11.2	0.8 ± 0.01
K6	21.9 ± 0.6	9.1 ± 0.1	414.7	320.1 ± 2.6	0.7 ± 0.004
K7	17.9 ± 0.6	6.4 ± 0.1	358.4	259.1 ± 10.4	0.7 ± 0.01
All data[d]	20.3 ± 0.03	8.7 ± 0.005	428.5	354.3 ± 17.9	0.75 ± 0.015

[a] ±SE of parameter estimate.
[b] Substrate concentration at which $v = 0.5$ V [25].
[c] Hill coefficient.
[d] Composite fit of all data (five to six kidneys each studied in duplicate).

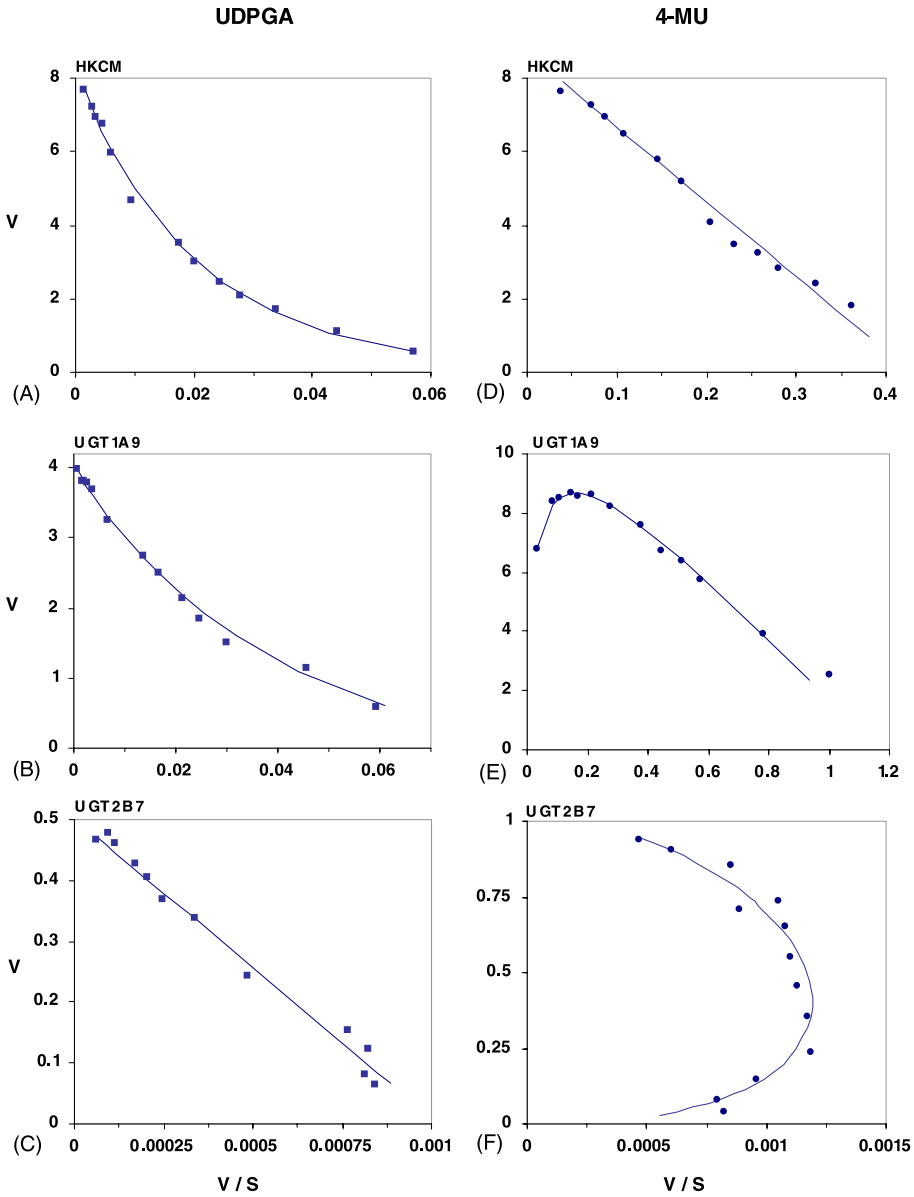

Fig. 1. Eadie–Hofstee plots for UDPGA and 4-MU glucuronidation catalysed by HKCM, UGT1A9 and UGT2B7. HKCM data for the co-substrate UDPGA (A) and 4-MU glucuronidation (D) are presented as mean of five to six kidneys, respectively, each studied in duplicate. Data for UGT1A9 (B and E) and UGT2B7 (C and F) are presented as the mean of duplicate determinations. Points are experimentally determined values, the solid lines show the computer derived curves of best fit.

4-MU glucuronidation (Fig. 2A) catalysed by HKCM (N = 5), or on UGT1A9 (Fig. 2B) or UGT2B7 activity (Fig. 2C). In contrast, unsaturated FA (C16:1–C20:5) inhibited significantly ($P < 0.001$) HKCM catalysed 4-MU glucuronidation in comparison to the control data (activity in the absence of FA) (Fig. 2A). Irrespective of the enzyme source (Fig. 2A–C), monoenoic FA from C16:1 to C20:1 inhibited 4-MU glucuronidation by 25–60% while increasing the degree of unsaturation (five double bonds) resulted in >70% inhibition (range 71–93%). The most potent inhibitor of HKCM, UGT1A9 and UGT2B7 catalysed 4-MU glucuronidation was C20:4, i.e. AA (Fig. 2A–C).

Investigation of the mechanism of inhibition was undertaken using the 'essential' FA LA (C18:2) and AA (C20:4) with either HKCM or UGT1A9 as the enzyme source. Studies were not conducted with UGT2B7 because of the inherent difficulties of studying inhibitory kinetics in the presence of sigmoidal substrate kinetics (Fig. 1F). Inhibition of 4-MU glucuronidation by HKCM was competitive for both FA, with respective apparent K_i values of 6.34 ± 0.08 μM and 0.15 ± 0.01 μM for LA and AA (Fig. 3A and B). Similarly, LA was a competitive inhibitor of 4-MU glucuronidation catalysed by UGT1A9 (apparent K_i 4.06 ± 0.26 μM, Fig. 3C). However, when using UGT1A9 protein, inhibition of

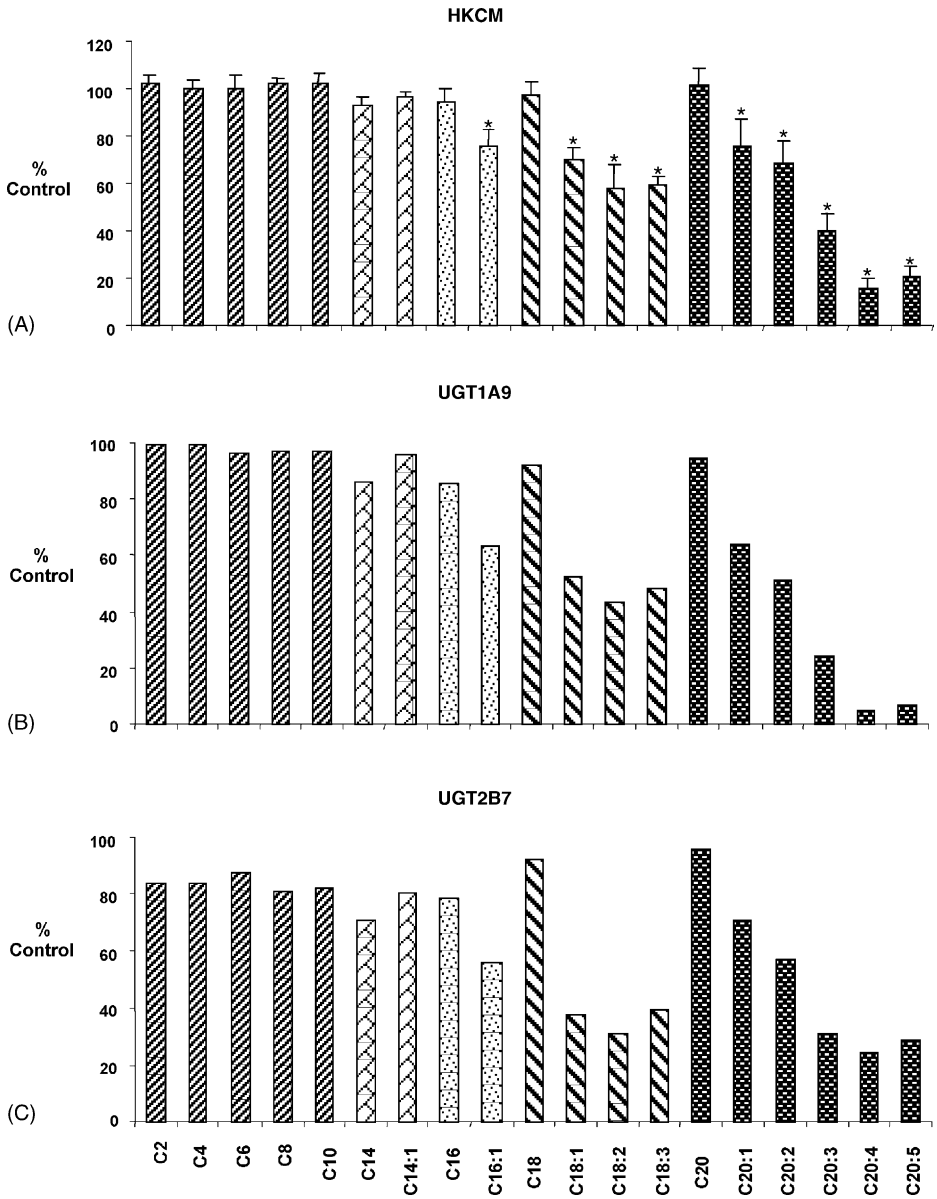

Fig. 2. Effect of FA (C2–C20:5) on 4-MU glucuronidation catalysed by HKCM, UGT1A9 and UGT2B7. Results are presented as percent of control activity (in the absence of fatty acid) ±SD from five individual kidneys (HKCM) each studied in duplicate (A). Data for UGT1A9 (B) and UGT2B7 (C) are presented as mean of duplicate determinations. Statistical significance is denoted as $^{*}P < 0.001$.

4-MU glucuronidation by AA exhibited atypical kinetics (Fig. 3D).

4. Discussion

This study has demonstrated that 4-MU glucuronidation activity in HKCM (CL_{int} 428.5 μL/min/mg) is directly comparable to that reported previously for 4-MU glucuronidation by human liver microsomes (CL_{int} 413.8 μL/min/mg) [24]. Recent studies have also reported comparable activity between human liver and human kidney microsomes for the glucuronidation of mycophenolic acid [16] and propofol [27]. Although extrapolation of *in vitro* kinetic parameters (using appropriate scaling factors) indicates that the contribution of the kidney to glucuronidation clearance *in vivo* is likely to be minor in comparison to the liver [28], these data nevertheless suggest that renal UGTs have an important 'local' detoxification role in the kidney. Indeed due to the concentrative action of renal transporters and the reabsorption of water, the urine concentration of many drugs and their metabolites may be higher than their respective plasma concentrations. Given the critical role of the kidney in drug and xenobiotic excretion the presence of UGT and other xenobiotic metabolising enzymes may assume major significance for protection against drug-induced nephrotoxicity.

Renal ischaemia resulting from either extra- or intra-renal factors accounts for approximately 50% of all cases of acute renal failure and is associated with the development

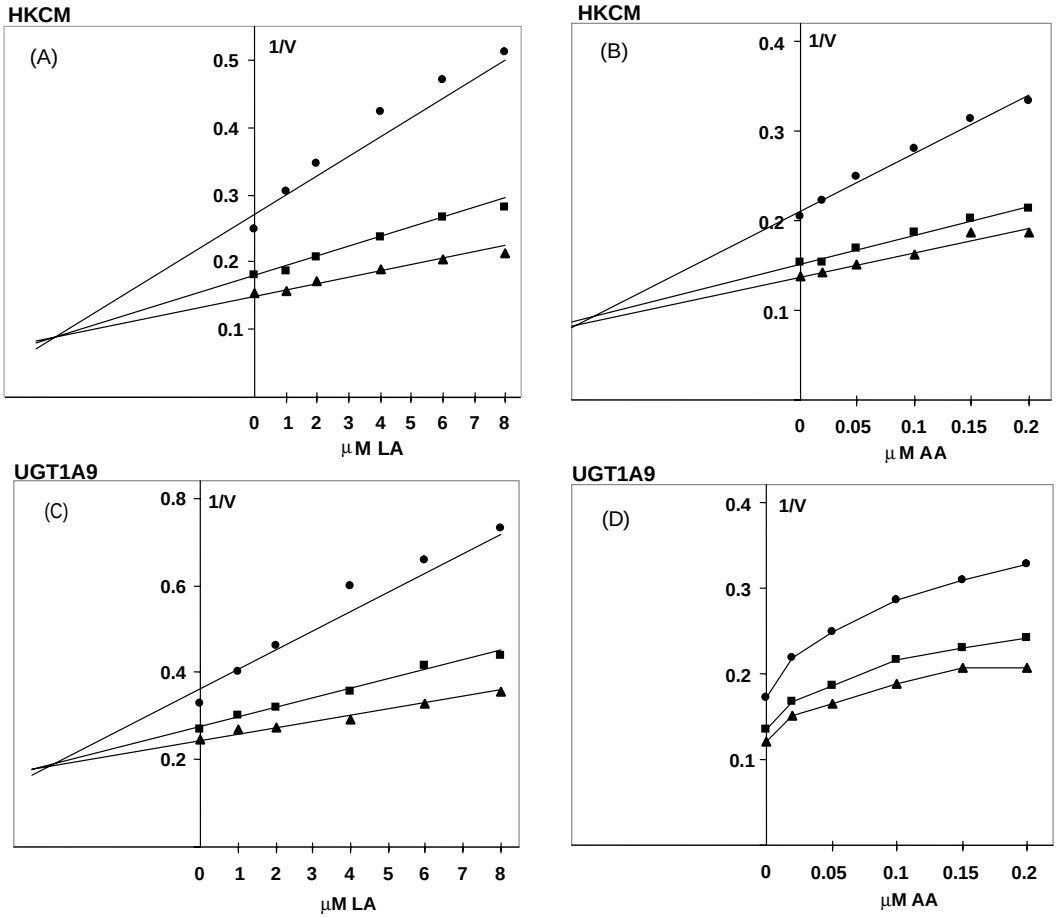

Fig. 3. Dixon plots for inhibition of 4-MU glucuronidation catalysed by HKCM and UGT1A9. Inhibition by LA (A, 1–8 μM) and AA (B, 0.02–0.2 μM) was studied using HKCM (N = 3 kidneys studied in duplicate) in the presence of 20 (●), 40 (■) or 60 μM (▲) 4-MU. Linoleic and AA inhibition of 4-MU glucuronidation catalysed by UGT1A9 using 10 (●), 20 (■) or 30 μM (▲) 4-MU are shown in C and D. Data represent mean of duplicate determinations. Note the atypical kinetics observed with AA (D). Points are experimentally determined values (A–D), the solid lines show the computer derived lines of best fit (A–C).

of significant biochemical alterations [29]. These include mobilisation of AA, accumulation of free FA, long-chain acyl carnitines and long-chain acyl coenzyme A esters, and decreased β-oxidation in both mitochondria and peroxisomes [30–32]. Given the high therapeutic concentration of long-chain FA that accumulate in renal ischaemia we investigated the effect of saturated and unsaturated FA on renal UGT activity. 4-MU is a non-selective UGT substrate and therefore represents a convenient probe for comparing the glucuronidation activity of tissues and recombinant enzymes. Although the primary focus of this investigation was the effect of FA on renal UGT activity, aspects of 4-MU glucuronidation and UDPGA kinetics observed in these studies warrant discussion. Whereas 4-MU glucuronidation by HKCM exhibited single-substrate MM kinetics (K_m^{app} 20.3 μM), atypical kinetics were observed for UGT1A9 and UGT2B7. 4-MU glucuronidation by UGT1A9 fitted a 'weak' substrate inhibition model (K_m 10.2 μM, K_{si} 289.6 μM) while 4-MU glucuronidation by UGT2B7 exhibited positive homotropic cooperativity (s_{50} 440.6 μM, $h = 1.65$). By definition cooperative kinetics suggests that UGT2B7 has two binding sites for 4-MU.

Our data support a recent study that ascribed atypical kinetics for morphine-3, and morphine-6-glucuronidation by UGT2B7 to a multi-site model involving simultaneous binding of two substrate molecules acting in a negatively cooperative manner [33]. However, the results of the present studies and that of Stone *et al.* [33] contrast with previous reports that have suggested that UGT2B7 has one substrate binding site [34,35]. Evidence of kinetic data representing either 'one binding site' or 'two binding sites' highlights the complexity of kinetic mechanisms manifest by UGTs. Our study reports positive homotropic cooperativity with UGT2B7 when 4-MU is the substrate. This contrasts with the negative cooperativity observed with morphine as the substrate [33] and further contrasts with the single site MM kinetics observed with UGT2B7 when 5-hydroxyrofecoxib was the substrate [36]. The presence of two or more binding sites has also been suggested recently for UGT1A1 as kinetic data indicative of both single and multi-site interactions were observed for

estradiol-17 and estradiol-3-glucuronidation [37]. Clearly, the kinetics observed in the present study with recombinant UGT2B7 and those reported previously with UGT1A1 reflect unique interactions that are substrate specific. In addition, accumulating evidence also suggests that some active UGT isoforms exist as dimers, although the impact of dimerisation on the kinetics of UGT-catalysed reactions is unknown [38]. Thus currently, variability in the kinetic behaviour of UGT necessitates the selection of appropriate models for describing the kinetics of drug glucuronidation.

As discussed, evidence of non-hyperbolic substrate kinetics for UGT catalysed reactions is increasing. However, an additional complicating factor highlighted by this study is the apparent variability in UDPGA kinetics. Negative cooperativity ($h < 1$) was observed in this study for UDPGA kinetics determined in the presence of a fixed concentration of 4-MU and using UGT1A9 as the enzyme source (apparent s_{50} 88.2 μM). Like UGT1A9, biphasic UDPGA kinetics were observed with 4-MU as the 'second' substrate when using HKCM (apparent s_{50} 354.3 μM). A similar observation of biphasic UDPGA kinetics interpreted as a two MM model (K_m^{app} 40 and 143 μM) has been reported with human liver microsomes using 1-naphthol as the second substrate [24]. In contrast, linear UDPGA kinetics were observed with 4-MU using UGT2B7 (K_m^{app} 493.2 μM). Interestingly, using different sources of UGT protein (e.g. human liver microsomes, rat hepatocytes) and varying xenobiotic substrates an array of kinetics has been observed for the co-substrate UDPGA, for example, biphasic and linear kinetics with 1-naphthol and 4-MU, respectively [24] and mixed cooperativity with bilirubin [39]. However, this is the first report describing different UDPGA kinetic models for recombinant UGTs, negative cooperativity for UGT1A9, and hyperbolic kinetics for UGT2B7. Taken together, these observations clearly indicate that the initial phenomenological reports of non-MM kinetics for UGT catalysed reactions can equally occur when investigating the kinetics of either the primary substrate or the co-substrate (i.e. UDPGA).

Naturally occurring FA can be classed simply as saturated and unsaturated. In a general but not exclusive sense, the former are involved in energy storage while the latter influence the physical properties of membranes and are also involved in eicosanoid production. In this study, saturated FA (C2–C20) did not inhibit 4-MU glucuronide formation catalysed by either HKCM, UGT1A9 or UGT2B7. In contrast, increasing both the chain length and the degree of unsaturation of the FA from monounsaturated (e.g. C16:1) through to polyunsaturated (e.g. C20:5) resulted in substantial inhibition (25–93%) of 4-MU glucuronidation by HKCM, UGT1A9 and 2B7. Of interest was the substantial inhibition observed with AA and LA. The latter is an omega-6 FA precursor for the production of AA, which is known to accumulate during periods of renal ischaemia and is extensively metabolised to biologically active eicosanoids.

Further investigation of the inhibitory effects of the LA and AA established that LA was a potent competitive inhibitor of 4-MU glucuronidation by both HKCM and UGT1A9 with apparent K_i values 6.34 and 4.06 μM, respectively. AA was an order of magnitude more potent than LA as a competitive inhibitor of HKCM UGTs (apparent K_i 0.15 μM) but, unlike the competitive kinetics observed with LA, the kinetics of inhibition of UGT1A9 by AA were atypical. Establishing inhibitory constants for LA and AA using UGT2B7 was not undertaken because of the complexity of interpreting inhibitory kinetics in the presence of sigmoid substrate kinetics (observed with 4-MU). This precluded further studies investigating the mechanism of FA inhibition using UGT2B7. Significant glucuronidation activity has been reported for human kidney and in particular it has been proposed that the level of UGT2B7 may be comparable with that of liver [28]. It should be noted, however, that although both LA (K_m^{app} 124 μM) and AA (K_m^{app} 149 mM) are substrates for UGT2B7 [11,12] the apparent K_m values reported suggest that UGT2B7 may not be the predominant isoform glucuronidating FA in human kidney.

The results reported here indicate that, at physiologically relevant concentrations unsaturated FA are inhibitors of renal UGT activity. In this respect, LA and AA rank as the most potent endogenous inhibitors of UGT activity demonstrated to date [40]. Importantly, our data suggest that during periods of renal ischaemia FA may impair renal drug metabolism *via* glucuronidation thus potentially exposing the kidney to high concentrations of drugs and/or their metabolites. Although the *in vivo* significance of our data needs to be fully investigated, the premise underlying our findings is indeed appealing.

Acknowledgments

Thanks are due to Virginia Papangelis for coordinating renal tissue collection and Xiao Hui Guo for expression of recombinant UGT proteins. The research was supported by grants from the Flinders Medical Research Institute (K.M.K.) and the National Health and Medical Research Council of Australia (J.O.M.).

References

[1] Chawla A, Repa JJ, Evans RM, Mangelsdorf DJ. Nuclear receptors and lipid physiology: opening the X-files. Science 2001;294:1866–70.
[2] Calder PC, Zurier RB. Polyunsaturated fatty acids and rheumatoid arthritis. Cur Opin Clin Nutr Metab Care 2001;4:115–21.
[3] Gil A. Polyunsaturated fatty acids and inflammatory diseases. Biomed Pharmacother 2002;56:388–96.
[4] Zoja C, Perico N, Remuzzi G. Abnormalities in arachidonic acid metabolites in nephrotoxic glomerular injury. Toxicol Lett 1989;46: 65–75.
[5] Simopoulos AP. Essential fatty acids in health and chronic disease. Am J Clin Nutr 1999;70(Suppl 1):560S–9S.

[6] Pritchard M, Fournel-Gigleux S, Siest G, Mackenzie P, Magdalou J. A recombinant phenobarbital-inducible rat liver UDP-glucuronosyltransferase (UDP-glucuronosyltransferase 2B1) stably expressed in V79 cells catalyses the glucuronidation of morphine, phenols and carboxylic acids. Mol Pharmacol 1994;45:42–50.
[7] Green MD, Belanger G, Hum DW, Belanger A, Tephly TR. Glucuronidation of opioids carboxylic acid-containing drugs, and hydroxylated xenobiotics catalysed by expressed monkey UDP-glucuronosyltransferase 2B9 protein. Drug Metab Dispos 1997;25:1389–94.
[8] Green MD, King CD, Mojarrabi B, Mackenzie PI, Tephly TR. Glucuronidation of amines and other xenobiotics catalysed by expressed human UDP-glucuronosyltransferase 1A3. Drug Metab Dispos 1998;26:507–12.
[9] Jude AR, Little JM, Freeman JP, Evans JE, Radominska-Pandya A, Grant DF. Linoleic acid diols are novel substrates for human UDP-glucuronosyltransferases. Arch Biochem Biophys 2000;380:294–302.
[10] Jude AR, Little JM, Czernik PJ, Tephly TR, Grant DF, Radominska-Pandya A. Glucuronidation of linoleic acid diols by human microsomal and recombinant UDP-glucuronosyltransferases: identification of UGT2B7 as the major isoform involved. Arch Biochem Biophys 2001;389:176–86.
[11] Jude AR, Little JM, Bull AW, Podgorski I, Radominska-Pandya A. 13-Hydroxy- and 13-oxooctadecadienoic acids: novel substrates for human UDP-glucuronosyltransferases. Drug Metab Dispos 2001;29: 625–55.
[12] Sonka J, Little J, Samokyszyn V, Radominska-Pandya A. Glucuronidation of arachidonic acid, 20-hydroxy-eicosatetraenoic acid and prostaglandin E2 by human hepatic and intestinal UDP-glucuronosyltransferases and recombinant UGT2B7. Drug Metab Rev 2002; 34(Suppl 1):194.
[13] McGurk KA, Brierley CH, Burchell B. Drug glucuronidation by human renal UDP-glucuronosyltransferases. Biochem Pharmacol 1998;55:1005–12.
[14] Lohr JW, Willsky GR, Acara MA. Renal drug metabolism. Pharmacol Rev 1998;50:107–41.
[15] Soars MG, Riley RJ, Findlay KAB, Coffey MJ, Burchell B. Evidence for significant differences in microsomal drug glucuronidation by canine and human liver and kidney. Drug Metab Dispos 2001;29:121–6.
[16] Bowalgaha K, Miners JO. The glucuronidation of mycophenolic acid by human liver, kidney and jejunum microsomes. Br J Clin Pharmacol 2001;52:605–9.
[17] Tukey RH, Strassburg CP. Human UDP-glucuronosyltransferases metabolism expression and disease. Annu Rev Pharmacol Toxicol 2000;40:581–616.
[18] Turgeon D, Carrier JS, Levesque E, Hum DW, Belanger A. Relative enzymatic activity, protein stability, and tissue distribution of human steroid-metabolising UGT2B subfamily members. Endocrinology 2001;142:778–87.
[19] Beaulieu M, Levesque E, Hum DW, Belanger A. Isolation and characterization of a human orphan UDP-glucuronosyltransferase, UGT2B11. Biochem Biophys Res Commun 1998;248:44–50.
[20] Brash AR. Arachidonic acid as a bioactive molecule. J Clin Invest 2001;107:1339–45.
[21] Lowry OH, Rosebrough NJ, Farr AL, Randall RJ. Protein measurement with the Folin phenol reagent. J Biol Chem 1951;193:265–75.
[22] Hobbs S, Jitrapakdee S, Wallace JC. Development of a bicistronic vector driven by the human polypeptide chain elongation factor 1 alpha promoter for creation of stable mammalian cell lines that express very high levels of recombinant proteins. Biochem Biophys Res Commun 1998;252:368–72.
[23] Sorich MJ, Smith PA, McKinnon RA, Miners JO. Pharmacophore and quantitative structure activity relationship modelling of UDP-glucuronosyltransferase 1A1 (UGT1A1) substrates. Pharmacogenetics 2002; 12:635–45.
[24] Miners JO, Lillywhite KJ, Matthews AP, Jones ME, Birkett DJ. Kinetic and inhibitor studies of 4-methylumbelliferone and 1-naphthol glucuronidation in human liver microsomes. Biochem Pharmacol 1988;37:665–71.
[25] Cornish-Bowden A. Control of enzyme activity. In: Cornish-Bowden A, editor. Fundamentals of enzyme kinetics. London: Portland Press; 1995. p. 203–16.
[26] Boxenbaum HG, Riegelman S, Elashoff RM. Statistical estimations in pharmacokinetics. J Pharmacokinet Biopharm 1974;2:123–48.
[27] Raoof AA, van Obbergh LJ, de Ville de Goyet J, Verbeeck RK. Extrahepatic glucuronidation of propofol in man: possible contribution of gut wall and kidney. Eur J Clin Pharmacol 1996;50:91–6.
[28] Fisher MB, Paine MF, Strelevitz TJ, Wrighton SA. The role of hepatic and extrahepatic UDP-glucuronosyltransferases in human drug metabolism. Drug Metab Rev 2001;33:273–97.
[29] Thadhani R, Pascual M, Bonventre JV. Acute renal failure. N Engl J Med 1996;334:1448–60.
[30] Finkelstein SD, Gilfor D, Farber JL. Alterations in the metabolism of lipids in ischemia of the liver and kidney. J Lipid Res 1985;26: 726–34.
[31] Ruidera E, Irazu CE, Rajagopalan PR, Orak JK, Fitts CT, Singh I. Fatty acid metabolism in renal ischemia. Lipids 1988;23:882–4.
[32] Portilla D. Role of fatty acid beta-oxidation and calcium-independent phospholipase A2 in ischemic acute renal failure. Curr Opin Nephrol Hypertens 1999;8:473–7.
[33] Stone AN, Mackenzie PI, Galetin A, Houston JB, Miners JO. Isoform-selectivity and kinetics of morphine 3- and 6-glucuronidation by human UDP-glucuronosyltransferases: evidence for atypical glucuronidation kinetics by UGT2B7. Drug Metab Dispos 2003;31:1086–9.
[34] Rios GR, Tephly TR. Inhibition and active sites of UDP-sglucuronosyltransferases 2B7 and 1A1. Drug Metab Dispos 2002;30:1364–7.
[35] Coffman BL, Kearney WR, Green MD, Lowery RG, Tephly TR. Analysis of opioid binding to UDP-glucuronosyltransferase 2B7 fusion proteins using nuclear magnetic resonance spectroscopy. Mol Pharmacol 2001;59:1464–9.
[36] Zhang JY, Zhan J, Cook CS, Ings RM, Breau AP. Involvement of human UGT2B7 and 2B15 in rofecoxib metabolism. Drug Metab Dispos 2003;31:652–8.
[37] Williams JA, Ring BJ, Cantrell VE, Campanale K, Jones DR, Hall SD, Wrighton SA. Differential modulation of UDP-glucuronosyltransferase 1A1 (UGT1A1)-catalysed estradiol-3-glucuronidation by the addition of UGT1A1 substrates and other compounds to human liver microsomes. Drug Metab Dispos 2002;30:1266–73.
[38] Miners JO, Smith PA, Sorich MJ, McKinnon RA, Mackenzie PI. Predicting human drug glucuronidation parameters: application of in vitro and in silico modelling approaches. Annu Rev Pharmacol Toxicol 2004;44:1–25.
[39] Bruni S, Chang TMS. Kinetic studies of hepatocyte UDP-glucuronosyltransferase: evidence of an allosteric enzyme. Artif Cells Blood Substit Immobil Biotechnol 1999;27:343–56.
[40] Grancharov K, Naydenova Z, Lozeva S, Golovinsky E. Natural and synthetic inhibitors of UDP-glucuronosyltransferase. Pharmacol Ther 2001;89:171–86.